remote sensing

MDPI

Article

RAP-MAC: A Robust and Adaptive Pipeline MAC Protocol for Underwater Acoustic String Networks

Xiaohe Pan [1], Mengzhuo Liu [1], Jifeng Zhu [1], Lipeng Huo [1], Zheng Peng [2,*], Jun Liu [3] and Jun-Hong Cui [1,2,4]

[1] College of Computer Science and Technology, Jilin University, Changchun 130012, China; panxh18@mails.jlu.edu.cn (X.P.)
[2] Shenzhen Institute for Advanced Study, University of Electronic Science and Technology of China, Shenzhen 518110, China
[3] School of Electronic and Information Engineering, Beihang University, Beijing 100191, China; liujun2019@buaa.edu.cn
[4] Smart Ocean Technology Co., Ltd., Shenzhen 518057, China
* Correspondence: zheng.peng@uestc.edu.cn

Abstract: The development of underwater acoustic networks is a significant expansion of Internet-of-Things technology to underwater environments. These networks are essential for a variety of marine applications. For many practical uses, it is more efficient to collect marine data from a remote location over multiple hops, rather than direct point-to-point communications. In this article, we will focus on the underwater acoustic string network (UA-SN) designed for this type of application. We propose a Robust and Adaptive Pipeline Medium Access Control (RAP-MAC) protocol to enhance the network's transmission efficiency, adaptability, and robustness. The protocol includes a scheduling-based concurrent algorithm, online real-time configuration adjustment function, a rate mode adaptive algorithm, and a fault recovery algorithm. We conducted simulations to compare the new protocol with another representative protocol, validating the RAP-MAC protocol's adaptability and fault recovery ability. Additionally, we carried out two large-scale sea trials. The results of these experiments indicate that the RAP-MAC protocol ensures effectiveness and reliability in large-scale multihop UA-SNs. In the South China Sea, we were able to achieve a communication distance of 87 km with a throughput of 601.6 bps, exceeding the recognized upper bound of underwater acoustic communication experiment performance by 40 km·kbps.

Keywords: underwater acoustic string networks; robustness; adaptive; MAC

Citation: Pan, X.; Liu, M.; Zhu, J.; Huo, L.; Peng, Z.; Liu, J.; Cui, J.-H. RAP-MAC: A Robust and Adaptive Pipeline MAC Protocol for Underwater Acoustic String Networks. *Remote Sens.* **2024**, *16*, 2195. https://doi.org/10.3390/rs16122195

Academic Editor: Silvia Liberata Ullo

Received: 14 April 2024
Revised: 25 May 2024
Accepted: 5 June 2024
Published: 17 June 2024

1. Introduction

Water covers over 70% of the Earth's surface. Nonetheless, there is little knowledge of the underwater world, as most of it remains unexplored. To study the unknown, underwater communication and networking technology, as well as the equipment, have developed rapidly. Recently, the concept of Underwater Internet of Things has emerged as an influential tool for a variety of underwater applications [1]. Then, the quasi-real-time communication between underwater nodes and control centers can be achieved. Establishing an underwater acoustic network enables the surveillance and detection of specific marine areas and the collection of various types of marine data [2–6].

Among the wide variety of marine applications, underwater long-distance monitoring and data transmission are in high demand. This type of technology can be used for monitoring shallow sea environments with a complex terrain, such as islands and reefs. For instance, it is suitable for coastal environment and biological monitoring [7]. It can also be used for observing coastlines, surveilling subsea oil and gas pipelines, monitoring river courses, and transmitting data over long distances in shallow or deep seas [8–10]. Point-to-point underwater acoustic communication is insufficient for these applications because its transmission range and monitoring scale are limited. Achieving point-to-point underwater

acoustic communication over tens or hundreds of kilometers, or even longer distances, requires exceptionally high power, which places significant demands on hardware and could cause marine noise pollution, posing a threat to marine animals.

To meet the requirements of the aforementioned applications, the concept of Underwater Acoustic String Network (UA-SN) is introduced. The UA-SN consists of a remote terminal node (RTN), multiple forwarding nodes (FNs), and a gateway node (GN). In this network, the RTN collects and sends data, the FNs sequentially forward the data to the GN, and the GN uploads the data to the onshore data center through the RF channel. In addition, the GN can also forward instructions from the data center to an underwater node in this network. The number of nodes in the UA-SN can be determined based on the application requirements. And the network can be deployed in a straight line or a zigzag pattern depending on the terrain and practical considerations. Furthermore, with a given number of nodes, the string topology is able to cover the longest communication distance. In summary, the underwater acoustic string network plays an irreplaceable role in addressing the challenges of remote monitoring and data transmission in such applications.

To implement a practical and reliable real-world underwater acoustic string network, designing an effective Medium Access Control (MAC) protocol is vital. However, MAC protocol design faces many challenges [11–13]. First, underwater acoustic channels are considered to be highly challenging, characterized by low propagation speed, limited bandwidth, multipath, large Doppler effect, high noise, and spatio-temporal variability. These characteristics result in long propagation delay, low data rate, high bit error rate and unstable links in underwater acoustic communication [14,15]. Second, these aforementioned features bring high end-to-end delay, low delivery ratio, and topology changes to underwater networks. What is worse, underwater devices are susceptible to damage because of the harsh marine environment. If any hop link in the underwater acoustic string network is disrupted due to device failure, the entire network can become paralyzed. Given these challenging issues and considering the hardware constraints such as half-duplex, limited available bandwidth, and low computing power, the existing MAC protocols are insufficient in handling them effectively.

Therefore, we propose a Robust and Adaptive Pipeline MAC (RAP-MAC) protocol for UA-SNs. The RAP-MAC protocol is a cross-layer optimization approach that primarily focuses on four aspects: (1) adopting a scheduling-based concurrency algorithm to enhance the data transmission efficiency; (2) introducing the real-time control of network parameters to make the network more manageable, heightening the network's reconfigurability and controllability; (3) designing a rate-adaptive algorithm by incorporating physical layer modulation encoding mode based on channel quality to improve the reliability of single-hop transmission and the adaptability to changing underwater environments; (4) developing fault detection and network recovery algorithms based on the correlation between physical layer parameters. This ensures that if a node fails, the network can still self-recover, improving its fault tolerance. Overall, the main contributions of our work can be summarized as follows:

- In order to establish a practical UA-SN in real-world scenarios, taking into consideration the network features, channel characteristics and physical layer parameters, a systematic cross-layer optimized RAP-MAC is proposed. The RAP-MAC protocol design is characterized by four key highlights: parallel transmission method to prevent conflicts and improve network throughput, network regulation strategy to enhance the controllability of the network, cross-layer optimized rate adaptation algorithm to improve the adaptability to ever-changing ocean environment, and fault recovery algorithms to increase the network robustness. The comparative analysis with PMAC [16] through simulations confirmed the adaptive ability to environment changes and the fault recovery ability of RAP-MAC.
- Many existing research works on underwater networks are simulation-based, with few network systems conducting experiments in real ocean environments. In order to further validate the practicability of RAP-MAC, we established the UA-SN with

21 nodes in the selected areas of the North Sea and the South Sea of China for experiments respectively. The sea trial verification took nearly a month, during which we mobilized more than 40 people and 25 boats. Through a great deal of effort, the experimental results from two sea areas fully demonstrated good performance of the UA-SN using RAP-MAC from the abovementioned four aspects.

- The experiment result of a communication distance of 87 km and a throughput of 601.6 bps for UA-SNs is unparalleled. In our best effort, no other network systems in the current published research have achieved such a communication distance with such a comparable throughput. Furthermore, this achievement exceeds the recognized upper limit of underwater acoustic communication test performance by 40 km·kbps.

The remainder of this article is organized as follows. Section 2 introduces the related work in this field. Section 3 describes the application scenario and the network architecture. Section 4 gives details on the RAP-MAC protocol algorithm. Section 5 presents the simulation and ocean experiments of the underwater acoustic string network. Finally, Section 6 concludes the article and presents future work.

2. Related Work

The MAC layer is responsible for managing the access of each node to the shared channel to minimize collisions and extra overhead. The MAC protocols have a critical impact on the Quality of Service of underwater acoustic networks [17]. According to the access method of nodes, MAC protocols can be classified into three types: contention-free, contention-based and hybrid [18]. In this section, we will first provide an overview of MAC protocols in relation to UA-SNs, and then summarize the current state of real-world underwater network systems in terms of scale.

After conducting a survey on existing work, only the following MAC techniques have been found regarding the underwater acoustic string network. Luque-Nieto et al. propose an optimal fair scheduling Spatial-TDMA protocol for the underwater string sensor network, which exploits the large propagation delay to choose the best scheduling so as to achieve maximum throughput and network fairness [19]. A throughput-efficient TDMA transmission schedules technique is proposed [20]. If the physical link is reliable, this protocol can achieve high network throughput. Yang et al. propose a dual channel MAC protocol based on directional antenna (DADC-MAC), which increases the network coverage range, efficiently utilizes space, and reduces node interference compared to the omnidirectional antenna [21]. Nevertheless, this protocol necessitates directional antenna hardware support, and it becomes challenging to ascertain the direction of the node's transmission because underwater nodes will randomly rotate due to water flow. In [22], the throughput of linear unicast underwater networks is analyzed. And the researchers propose a general transmission scheduling strategy that can achieve the throughput upper bound and also give some examples of the optimal schedules. Son N. Le et al. propose a scheduling-based Pipelining MAC (PMAC) for underwater acoustic string networks [16]. This protocol is designed to take advantage of this topology: network nodes take turns to send, and those that are three hops apart are allowed to do so simultaneously, improving the throughput. Furthermore, the researchers performed comparative analysis on three representative MAC protocols—random access-based UW-Aloha [23], handshaking-based SASHA [24], and scheduling-based PMAC [6]—through sea trials [25].

The above methods mainly focus on improving throughput and do not consider the fact that the underwater acoustic link is spatiotemporally variable, vulnerable, and unreliable, and underwater nodes are prone to failures. When the channel deteriorates and leads to a high packet loss rate, if the protocol algorithm cannot effectively cope with it, the Quality of Service of the network will be greatly reduced. If the physical communication link is interrupted, the entire network segment between the remote terminal node and the interruption location will be completely disabled.

Through investigation on the actual deployment of underwater network systems both domestically and internationally, the sea trial network with a clear number of nodes is

summarized as follows. The US Navy's Seaweb program is an organized network for command, control, communications, and navigation of deployable autonomous undersea systems, comprised of fixed buoy nodes, underwater static nodes and underwater mobile nodes. The maximum number of nodes in the sea trial of this network system is 40, with nodes distributed within a range of 100–10,000 km^2 [26,27]. PLUSNet is also an underwater surveillance network program supported by the US Navy, which uses both fixed and mobile underwater platforms, including bottom nodes with detection systems, UUVs with towed arrays, and gliders with acoustic and environmental sensors. The number of PLUSNet sea trial nodes exceeds 50, with a monitoring range of hundreds of kilometers [28]. The UA-SN with nine nodes was deployed and tested about 100 miles offshore New Jersey in 2012. The end-to-end communication distance of this network is about 7.3 km [25]. The underwater network with four nodes, equipped with HEU OFDM-modems, was deployed to collect ocean environmental information in the South Sea, China, in 2014 [29]. To sum up, only the US Navy's Seaweb and PLUSNet have over 20 nodes and a coverage range of over 100 km.

In summary, despite the numerous studies on underwater networks, there are relatively few underwater networks that are actually used in real marine environments. In this article, to address practical application issues, we introduce the UA-SN architecture, and design and implement a systematic RAP-MAC protocol for this network, considering the aforementioned challenges. Additionally, a UA-SN with 21 nodes is built in real marine environments for protocol performance testing and the remote transmission of monitoring data. In the following section, we will present a concise description of network architecture scenarios and MAC protocol design issues.

3. Application Scenario and Network Architecture

Underwater acoustic networks, considered a promising network infrastructure, have wide application prospects in the marine field. For instance, stationary smart ocean observation network systems have been studied [30]. The application scenarios discussed in this article mainly concentrate on underwater bidirectional remote control and data transmission, for example, the environmental monitoring of inshore shallow sea with complex terrain, leakage detection and corrosion monitoring in underwater oil and gas pipelines, as well as deep-sea long-distance data transmission and control. The above applications cannot be satisfied solely by point-to-point underwater acoustic communication. Typically, underwater acoustic networks are organized as a multihop relay structure when they encounter these scenarios. And such underwater networks need to have the following functions: information acquisition in the uplink and command control in the downlink.

Given the aforementioned actual application requirements, the scalable underwater acoustic string network with multihop architecture has been introduced. This network, shown in Figure 1, is composed of one remote terminal node (RTN), a variable number of forwarding nodes (FNs) and one gateway node (GN). The UA-SN is capable of determining the number of underwater nodes and the deployment pattern (either a straight line or zigzag), depending on the terrain and practical demand. In UA-SN, the sensor information collected and dispatched by the remote terminal node is forwarded hop by hop by relay nodes and finally received by the gateway node, which then delivers it to the data center. The gateway node can also transmit commands from the data center to underwater nodes through the downstream underwater acoustic link. In addition to the data forwarding function, relay nodes can also be equipped with sensors for data collection and transmission.

In order to meet the practical needs of underwater acoustic string networks, it is crucial to design an effective MAC protocol. For such networks, the issues that the MAC protocol needs to take into account mainly manifest in the following aspects:

- Efficiency: how to effectively organize the data transmission of each node to avoid data conflicts, while maximizing network throughput;
- Reconfigurability: how to improve the network's flexibility, scalability, and controllability;

- Adaptability: how to enhance the network's adaptability to different underwater environments;
- Robustness: how to ensure network connectivity in the event of node failures or link interruptions.

Next, we will discuss the strategies to tackle these issues in the MAC protocol algorithm.

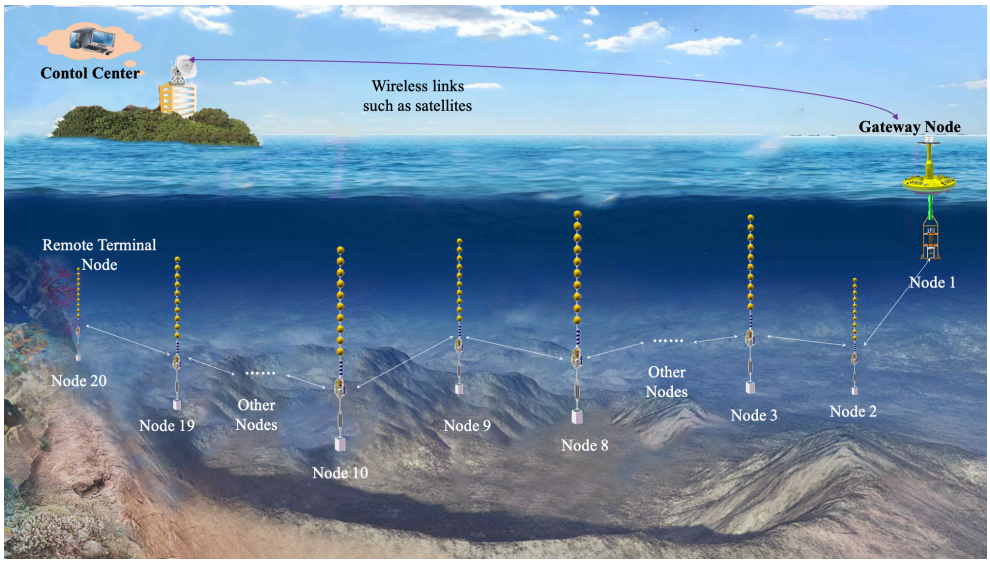

Figure 1. The UA-SN architecture.

4. Design of RAP-MAC

Taking into account the amount of time, manpower, resources, and financial costs needed to build an UA-SN that supports long-distance data transmission in a real marine environment, as well as the difficulty of network maintenance in case of failures, it is essential to fully consider the transmission efficiency, flexibility, controllability, adaptability, and robustness of the network during the design phase in order to increase its resilience. Consequently, the design details of the RAP-MAC protocol are described from four aspects.

4.1. Efficient, Reliable, and Conflict-Free Data Transmission Strategies

To deal with this issue, we have referred to the basic principles of our team's previous work, PMAC, as depicted in Figure 2. PMAC is a time division-based MAC protocol, which assumes that any two nodes that are geographically adjacent can receive each other's acoustic signals, while nodes that are not adjacent cannot. Thanks to the spatial characteristics of network deployment, the PMAC protocol allows for two nodes located three hops away from each other to transmit data simultaneously without causing collisions. This is demonstrated in the example of nodes 1 and 4. The protocol consists of two phases: the network establishment phase and the data transmission phase. During the former, the slot allocation strategy and the synchronization of the network start time are determined, whereas the latter involves each node sending data in its designated time slots. The time slot length is calculated by adding the maximum propagation delay between any two adjacent nodes and a preset data transmission delay. In the network establishment phase, the slot length is estimated on a per-hop basis, spreading from one end of the string network until the other end is reached. After determining the maximum propagation delay and the time slot length, the tail node selects a start time for the time slot and notifies the previous node of the time slot length and start time within its own time slot, allowing the previous node to synchronize the network start time and determine the time slot it will use. This process continues until it reaches the head node, completing the network establishment phase. During the data transmission phase, each node sends data in its designated time slots and uses an implicit acknowledgment mechanism (except for the

gateway node using an explicit ACK), which means that when the relay node forwards data, its previous hop node can check if the data transmission is successful by listening, minimizing control packet exchanges, and reducing energy consumption.

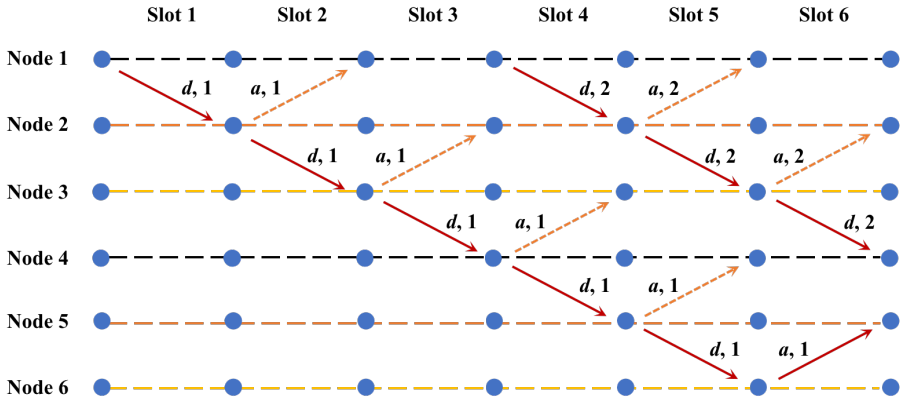

Figure 2. Example of protocol timing sequence scheduling. (*d* is the sending data, and *a* is listening to the forwarding data, i.e., implicit acknowledgment.)

4.2. Strategies to Improve the Reconfigurability

In order to improve the flexibility and controllability of the UA-SN, considering that the network deployment process may take a long time in practice, and to save energy, an instant control function for establishing network is designed. The gateway node is designated as the initiator for establishing a network. This enables the gateway node to initiate the time slot calculation after all nodes have been successfully deployed, avoiding the situation where some nodes in the network have not been deployed yet but remote terminal node has already started the time slot calculation, which could result in extra energy waste. Furthermore, considering the scalability of the network, when there is a temporary increase or decrease in nodes in the network, the network can be re-established and the time slot allocation for each node can be reconfigured in a timely manner. For PMAC UA-SNs, any change in the number of network nodes requires manual intervention to rebuild the network, with a complexity of O(n). All the configurations of UA-SNs in the proposed method can be accomplished autonomously.

To facilitate the smooth and efficient transmission of network data, we have made improvements to the data transmission phase of the PMAC protocol. We added controls for the start and pause of data transmission, as well as the frequency and length of data transmission. The control for data transmission start and pause allows for the suspension of data transmission when network re-establishment is required, and then resuming it after the successful re-establishment. The start and pause of data transmission are initiated by the gateway node. When network re-establishment is needed, the gateway node sends a Data Transmission Pause (DTP) control packet to all nodes in the network. Upon receiving the DTP packet, the nodes stop data transmission and forward DTP to the remote terminal node hop by hop. Then, the gateway node starts to establish the network. Once the network is successfully established, the gateway node sends a Data Transmission Start (DTS) packet to the remote terminal node to initiate data transmission. The frequency of data transmission can be adjusted to prevent network congestion when the packet loss rate is high in harsh underwater environments, and shortening the length of the data packets can also improve the transmission success rate.

4.3. Strategies to Enhance Adaptability to Dynamic Environments

The underwater acoustic channel exhibits strong temporal variability and is highly susceptible to the environment. For example, there are significant differences in the sound speed profile in summer and winter, which can cause changes in the propagation distance. Various sea conditions can also have a significant impact on the quality of the received

signals. The hydrological environment and sea conditions vary throughout the day, as well as in different oceans. Consequently, it is essential to enhance the adaptability of UA-SNs to different underwater environments, thereby improving their reliability and increasing the application value.

The RAP-MAC algorithm conducts cross-layer optimization in conjunction with the physical layer to enhance the adaptability of network nodes to the dynamic underwater acoustic channel. To enhance the reliability of underwater acoustic communication, the physical layer has designed multiple communication modes, which have different modulation and coding schemes with different rates. They are described as follows: the physical layer adopts OFDM (Orthogonal Frequency Division Multiplexing) modulation; each data packet contains a preamble and multiple data blocks, which can be up to 16; and guard intervals are inserted between the preamble and data blocks, as well as between data blocks (the guard interval can be set to 0.05 s/0.1 s/0.15 s). The calculation formula for the physical layer data rate (DR) is as follows:

$$DR^i = \frac{N_P \cdot M_b^i \cdot R_c^i}{\frac{N_S}{BW} + T_g}, \tag{1}$$

where $i \in [1, 2, 3, 4, 5]$ corresponds to the five rate modes of the physical layer, N_S is the total number of subcarriers, N_P is the number of data subcarriers, BW is the communication bandwidth, T_g is the guard interval, M_b^i is the number of bits modulated on each subcarrier at mode i, and R_c^i is the coding rate. Table 1 provides the rates for different communication modes, with BPSK modulation used at Mode 1, QPSK used at Modes 2 and 3, and 16QAM used at Modes 4 and 5.

Table 1. Communication rate at different modes.

Rate Mode		1	2	3	4	5
M_b^i		1	2	2	4	4
R_c^i		1/2	1/2	3/4	1/2	3/4
DR^i (kbps)	$T_g = 50$ ms	1.522	3.045	4.568	6.090	9.136
	$T_g = 100$ ms	1.241	2.482	3.724	4.965	7.447
	$T_g = 150$ ms	1.047	2.095	3.143	4.191	6.287

Under the Additive White Gaussian Noise (AWGN) channel, the relationship between the Block Error Rate (BLER) and Signal-to-Noise Ratio (SNR) for the five communication modes in Table 1 is shown in Figure 3.

By mapping the relationship between different communication modes, BLER and SNR from Figure 3 to a list, we can select the highest rate mode that meets the condition of a BLER not exceeding 0.05, based on the calculated SNR of the received signal, which ensures reliability while maximizing the network throughput. The formula for calculating SNR is as follows:

$$SNR_v = \frac{E_{k \in S_P}\{|z_v[k]|^2\} - E_{k \in S_N}\{|z_v[k]|^2\}}{E_{k \in S_N}\{|z_v[k]|^2\}}, \tag{2}$$

where $z_v[k]$ is the frequency observation at subcarrier k on the v-th hydrophone, S_P is the set of pilot subcarriers, and S_N is the set of null subcarriers.

Upon receiving data from the previous hop node, each node calculates the SNR of the received signal. The calculated SNR is then inserted into the forwarded data packet. When the previous hop node listens to the forwarded data, it will extract the SNR to adjust its own communication mode for sending data.

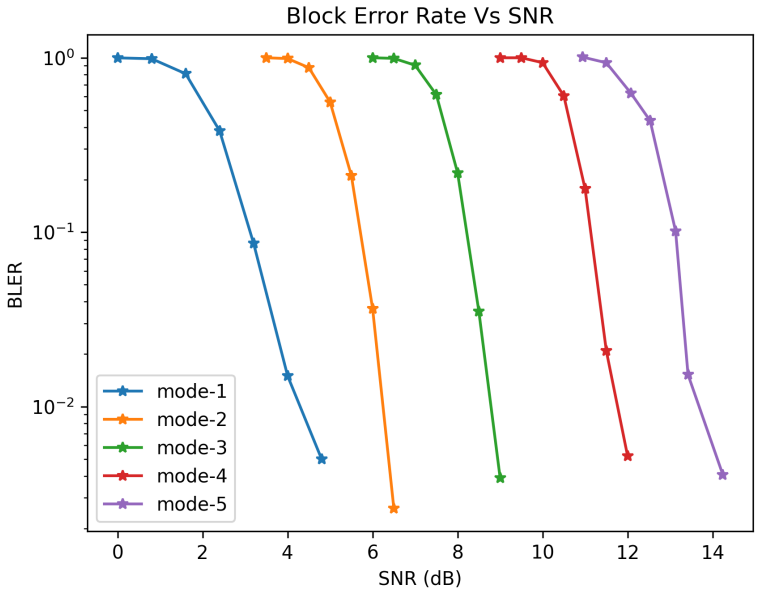

Figure 3. The relationship between BLER and SNR at different modes.

4.4. Strategies to Improve Robustness

As the number of nodes increases in a UA-SN, the end-to-end connectivity decreases. If any node fails or a segment of the link is interrupted, the data from subsequent nodes cannot be successfully transmitted. Manually detecting and locating faults and replacing equipment is time-consuming and difficult. Therefore, it is important to enhance the network's fault recovery capability to ensure end-to-end connectivity in UA-SNs and reduce maintenance costs. In order to detect node failures or link interruptions and cope with those in a timely manner, we will provide a detailed description of the RAP-MAC fault localization and network recovery algorithm.

Premise: to improve the throughput and link reliability of the network, the deployment distance of adjacent nodes is selected based on the highest rate mode (with a BLER not exceeding 0.05) achievable at this distance. In other words, the deployment distance for a single hop is smaller than the maximum communication distance D_{max} achievable in the lowest rate mode (i.e., $2D_{deploy} \leq D_{max}$). At the same time, the node's transmission power is controlled to not interfere with the data reception of its two-hop neighboring nodes. For example, according to the data transmission scheduling algorithm, Nodes 1 and 4 can simultaneously send data, and then the transmission power of the nodes is controlled to ensure that the data signal from Node 1 does not affect the signal reception of Node 3, and the data signal from Node 4 does not disrupt the signal reception of Node 2.

If an FN (such as Node 6 in Figure 1) forwards data to the next hop node in its time slot but does not receive any data signal forwarded by its next hop node in the following time slot, it will retransmit the data in its own time slot. If it still does not receive any forwarding signal from the next hop node in the next time slot, the FN will repeat this process once. If the FN fails to receive any forwarding signal for three consecutive times, then its next hop node (i.e., Node 5 in Figure 1) is considered faulty. When this situation occurs, in order to ensure that the entire network remains connected, we adopt a method of reducing the communication rate at the expense of network throughput to increase communication distance to directly bypass the faulty node and reach its next hop (i.e., Node 6 directly forwards data to Node 4, bypassing the faulty Node 5). When Node 6 detects the failure of Node 5, it first notifies the RTN to stop sending data to avoid data congestion at Node 6, and then proceeds with further processing. In order to reduce energy consumption, Node 6 will use a lower rate mode than its original mode. Under the condition that the BLER is not higher than 0.05, the SNR is calculated based on the relationship shown in Figure 3. Finally, the required sound power level is determined by using Formula (3) to adjust the transmission power of Node 6:

$$SPL_{TX} = SNR + N_O + Atten - OCRR, \tag{3}$$

where SPL_{TX} is the sound power level, N_O is the ocean ambient noise, $Atten$ is the propagation loss (including absorption loss and spreading loss), and $OCRR$ is the receiving response of the receiver transducer, a constant. $Atten$ is related to the propagation distance, and its calculation formula is as follows:

$$Atten = 20lg(D) + 10lg(\frac{L}{D}) + \alpha L, \tag{4}$$

where αL represents absorption loss, α is the absorption coefficient, and L is the propagation distance. The remaining part of the formula represents spreading loss, where D is the water depth. Spreading loss is related to the propagation model of sound waves. The spherical propagation attenuation radius is equivalent to the water depth, followed by cylindrical attenuation.

After adjusting the power, Node 6 sends a connectivity test packet (Ping) to Node 4, which includes the transmission power and communication mode parameters. Node 6 then waits for Node 4 to respond with a reply packet (Reply) using the same transmission power and communication mode. If Node 6 does not receive a reply within three time slots, it repeats this process. If there is still no reply after three attempts, Node 6 increases the transmission power and repeats the process until it receives feedback from Node 4.

The parameter adjustment rule for Node 6 is as follows: first, decrease the rate mode, and then adjust the power. If the power reaches its maximum and the connectivity still fails, decrease the rate mode once more. Calculate the minimum transmission power based on Formulas (3) and (4), and gradually increase the power until the connectivity test is successful. After successful connectivity between Node 4 and Node 6, during data transmission, Node 4 sends an extremely short Tone packet (with no payload) to explicitly acknowledge the data forwarded by Node 6, and continues to forward the data to the next hop using the original power and mode. However, due to the interference at Node 2 caused by the adjusted transmission parameters of Node 4, and to avoid conflicts, the transmission delay of the data should not exceed the propagation delay. Since Node 5 is faulty, so as to minimize time wastage, Node 6 sends a Re-establish Network Packet (RNP) to the gateway node, which includes information about the maximum length of data packets allowed to be sent. Upon receiving the RNP, the GN initiates network establishment, including the maximum packet length information. Once the network is successfully established, the GN sends a data transmission start packet to the RTN. The entire network then resumes normal operation. The algorithm flow is shown in Figure 4.

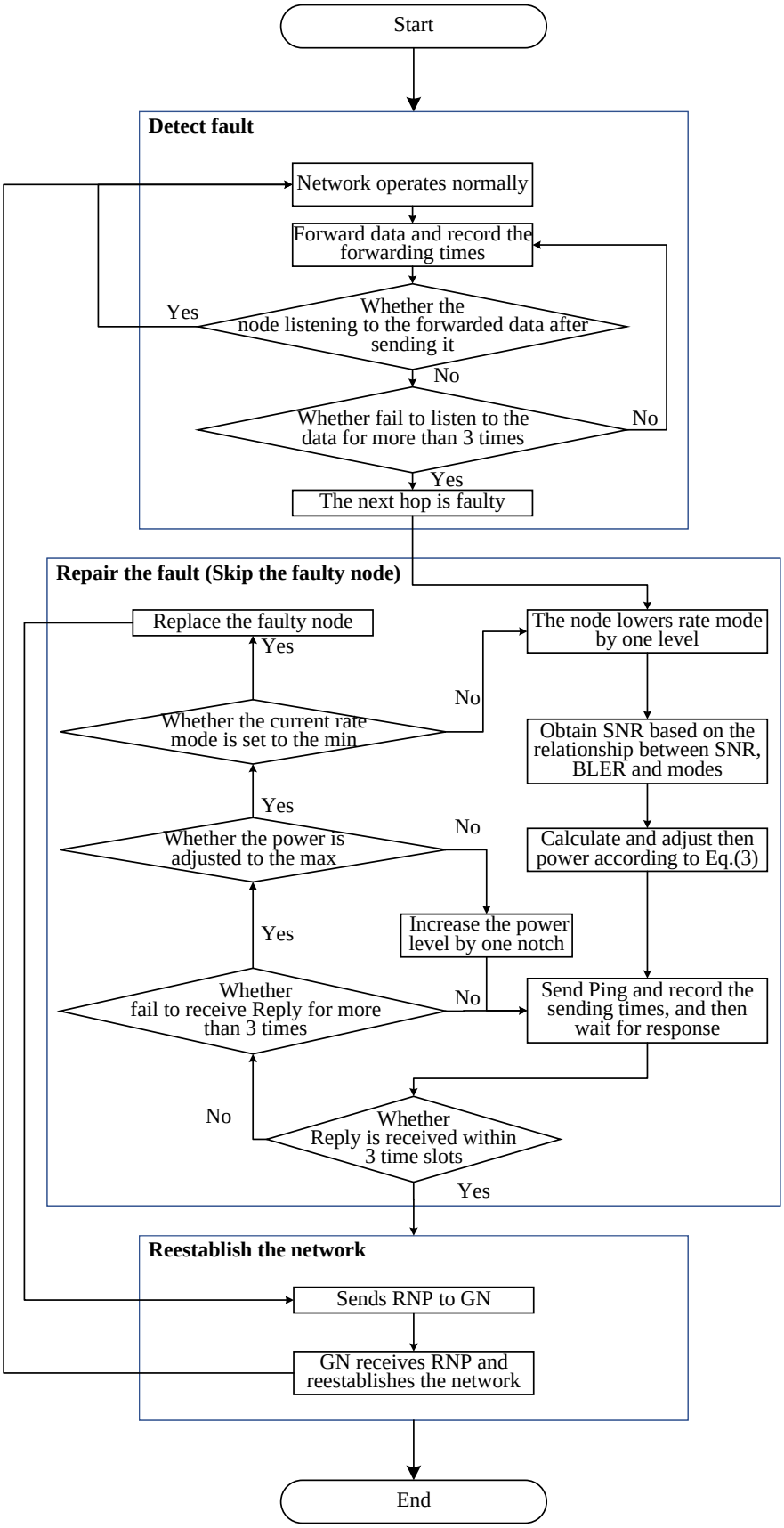

Figure 4. The flow of the fault recovery algorithm.

5. Experiments and Results

In this section, we first conduct simulations to compare the RAP-MAC with the PMAC. Following that, we implement the RAP-MAC protocol in practical systems and establish a 21-node UA-SN in different seas of China respectively. This is performed to thoroughly demonstrate the adaptability and robustness of the long-distance string network using the RAP-MAC protocol in different environments.

5.1. Performance Metrics

To evaluate the proposed MAC protocol's efficiency in data transmission, adaptability to different environments, and the network robustness in UA-SNs, this manuscript mainly employs network throughput and end-to-end data delivery ratio as performance metrics.

The network throughput is defined as the total amount of data successfully received by the gateway node per unit of time, denoted as $S = \frac{L_{data}}{Duration}$. Here, *Duration* represents the testing time period, and L_{data} is the total length of successfully received data during that time period. In the case where there is no packet loss, and each node is not idle in its own time slot, according to the algorithm design principle, and the throughput is the ratio of the length of a data packet to three time slots.

The end-to-end data delivery ratio is defined as the ratio of the number of data packets successfully received by the gateway node to the number of data packets sent by the remote terminal node, denoted as $D = \frac{n_r}{n_s}$. Here, n_r represents the number of data packets successfully received by the GN, and n_s is the number of data packets sent by the RTN.

5.2. Simulation Experiments

This subsection first introduces the implemented simulation platforms, followed by a description of two types of simulation experiment designs based on simulation platforms. Finally, an analysis of the simulation results is presented.

(1) Simulation Platforms

This article implements a simulation platform based on MATLAB and an Aqua-Net Mate simulation platform [31] based on the Bellhop physical channel. These two simulation platforms complement each other. Next, we will provide a more comprehensive introduction to these two simulation platforms.

- The simulation platform based on MATLAB is more flexible and allows for convenient parameter adjustments. The communication parameters at the physical layer are set based on the five rate modes provided in Section 4. The channel parameters are configured based on statistical data from sea trials. The main purpose of this simulation platform is to confirm the adaptability of the UA-SN using the RAP-MAC protocol in different underwater environments.
- The Aqua-Net Mate simulation platform based on the Bellhop model is specifically designed for underwater acoustic networks. We embed the Bellhop-based underwater acoustic channel model into this platform, using actual channel parameters and hydrological environments from field trials as inputs to make the simulation closer to real-world conditions. This simulation platform is primarily used to verify the fault recovery capability of the UA-SN using the RAP-MAC protocol.

In both simulation experiments, there are 21 network nodes, in which one end node serves as the data source node, while the other end node serves as the data receiving gateway node, and the intermediate nodes act as forwarding nodes. All nodes are deployed in a straight line, with a distance of 2 km between any adjacent nodes. The total end-to-end communication range is 40 km. The slot length is the sum of the propagation delay, data transmission delay and guard time. Based on the description of different rate modes in Section 3, the transmission delay of the longest data packet (including 16 data blocks) at various modes is consistent, approximately 6.0 s (with a delay of 0.17 s for each data block, a guard interval of 0.15 s between data blocks, a delay of 0.48 s for the preamble, and an extra processing delay of 0.4 s). The average speed of sound in water is 1500 m/s, so the

propagation delay is approximately 1.3 s. The guard time is set to 1.0 s, resulting in a slot length of 8.3 s.

(2) Experiments for Environmental Adaptability

Simulation Design: The simulation experiment is conducted using a MATLAB-based simulation platform. After conducting a continuous 3-day communication experiment in the Dalian area of the North China Sea in late May, we gathered data on the variation of SNR with respect to the environment during different periods of the day. The SNR values were recorded, and their average was calculated every 2 h. The results are shown in Figure 5, which displays the SNR information for 11 segments. Referring to the relationship between the mode, BLER and SNR in Figure 3 of Section 4, and considering the need to save simulation time and reduce unnecessary consumption, we further divided the SNR variation into four periods: 0:00–8:00 (average SNR of 11.3 dB), 9:00–12:00 (average SNR of 9.6 dB), 13:00–16:00 (average SNR of 8.5 dB), and 17:00–24:00 (average SNR of 9.5 dB), which are the configurations of the physical layer SNR parameters in the simulation platform. The data-sending period for the RTN is every three time slots. The length of the data packets is adaptively adjusted based on the selected rate mode. For Mode 1, the packet length is 600 B; for Mode 2, it is 1250 B; for Mode 3, it is 1950 B; and for Mode 4, it is 2600 B. With this configuration, we simulate the throughput and end-to-end delivery ratio variations of the UA-SN using the RAP-MAC during different periods of a day. We also simulate the throughput and end-to-end delivery ratio of the UA-SN using PMAC during the four periods, with each period using four different modes.

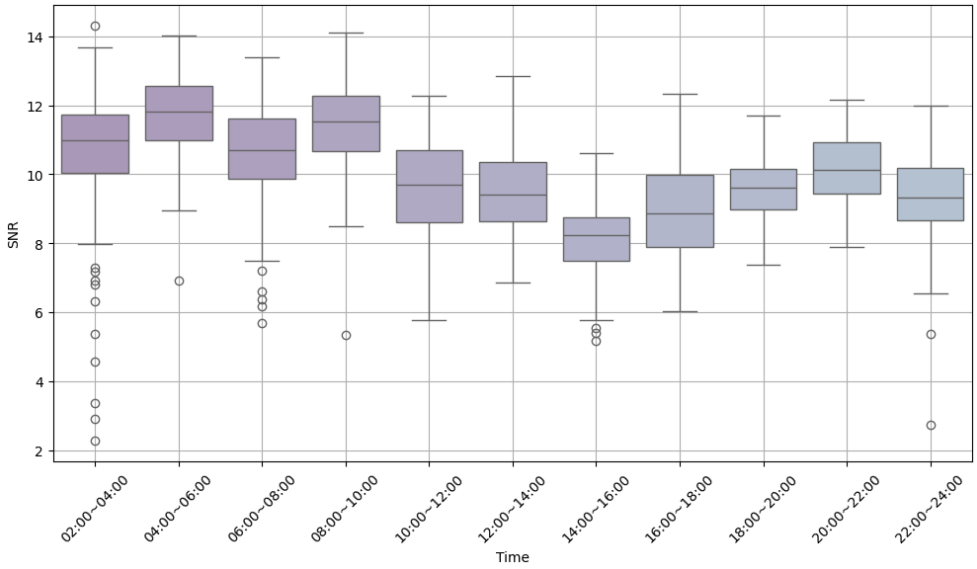

Figure 5. The SNR of during different periods of a day at communication range 2 km. (This is a box-plot, taking the data from 2:00 to 4:00 as an example. The lower boundary is 8, the upper boundary is 13.6, the 1st quartile is 10, the 2nd quartile is 11, and the 3rd quartile is 11.8. The small circle represents the outliers.)

Simulation Results: The simulation experiment results are shown in Figure 6 and Table 2, where the SNRs of 9:00–12:00 and 17:00–24:00 are almost the same, resulting in identical simulation results. From Figure 6, it can be observed that the UA-SN using the RAP-MAC algorithm can adapt to the optimal rate mode according to the environmental changes to improve network throughput during the four time periods. Since we conducted simulation tests on the UA-SN using PMAC with four different modes for each time period, we can see from the figure and table that there is always a communication mode in which the throughput and end-to-end delivery ratio results match those of the UA-SN using RAP-MAC. This confirms that the RAP-MAC algorithm improves the adaptability of UA-SNs to changing underwater environments.

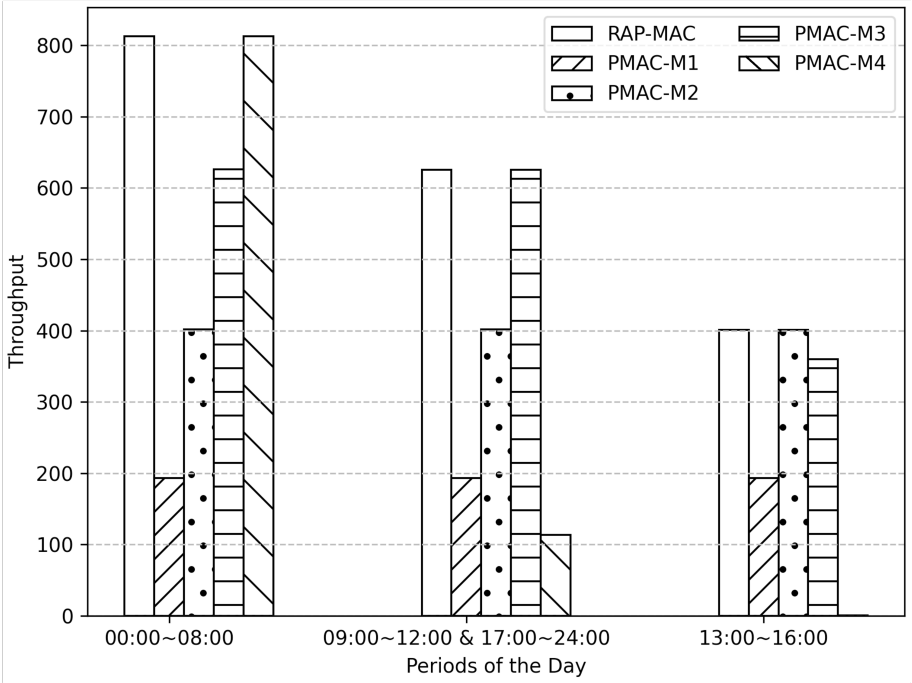

Figure 6. The throughput comparison.

Table 2. The end-to-end delivery ratio comparison.

Time Period	RAP-MAC	PMAC-m1	PMAC-m2	PMAC-m3	PMAC-m4
0:00–8:00	99.2%	99.9%	99.9%	99.9%	99.2%
9:00–12:00 & 17:00–24:00	99.9%	99.9%	99.9%	99.9%	15.2%
13:00–16:00	99.9%	99.9%	99.9%	98.2%	1.3%

Analysis of data transmission efficiency: From Figure 6, it can be observed that the optimal rate modes adapted by RAP-MAC in the morning, noon, and afternoon are Mode 4, Mode 3, and Mode 2, respectively. The corresponding throughputs are 820 bps, 630 bps, and 400 bps. Based on avoiding conflicts and without considering propagation delay and guard time overhead, the theoretical transmission rates for Mode 4, Mode 3, and Mode 2 are 1156 bps, 867 bps, and 556 bps, respectively. By comparing the theoretical transmission rates with the actual network throughput, it can be concluded that the actual transmission efficiency of the network is approximately 71% when considering the overhead of propagation delay and guard time.

(3) Experiments for Fault Recovery Capacity

Simulation Design: The simulation experiment is conducted using the Aqua-Net Mate simulation platform based on the Bellhop channel model. To make the simulation environment closer to reality, we use the hydrological environment of the Daya Bay area of the South China Sea as a reference. The average water depth is 15 m, and the node deployment depth is 7 m. The hydrological environment parameters are based on the sound speed profile data measured by the Sound Velocity Profiler (SVP) during sea trials. The seabed sediment is assumed to be clay, and the channel simulates the multipath, Doppler, and noise in sea trials. All of these configurations help to align the simulated environment more closely with real marine scenarios. The data transmission period for the RTN is every three time slots, with a data packet length of 1950 B. When a fault occurs, the packet length is self-adjusted according to the fault recovery algorithm. The probability of a node failure in the network is set to p, with p gradually increasing from 0% to 30%. The simulation evaluates the throughput and end-to-end delivery ratio of the UA-SN under the RAP-MAC and PMAC protocols.

Simulation Results: The simulation experiment results are illustrated in Figures 7 and 8. From Figure 7, it can be seen that the throughput of both MAC algorithms decreases as the fault probability increases. However, PMAC has a lower throughput compared to RAP-MAC. This is because when a fault occurs, the PMAC protocol cannot recover on its own, and the network is directly interrupted, resulting in a throughput of 0 after the network interruption. Thus, this leads to a lower overall average throughput. On the other hand, the proposed RAP-MAC algorithm can recover the network by skipping the faulty node through rate mode reduction when a fault occurs, resulting in a higher average throughput. However, after the network recovers, not only the rate mode is reduced but the allowed packet length is also significantly shortened, resulting in a significant decrease in throughput compared to before the fault. Assuming that Node 5 fails, according to the RAP-MAC protocol algorithm rules, Node 4 needs to skip Node 5 and directly connect to Node 6. Since Nodes 4 and 7 can send data simultaneously, in order to avoid conflicts at Node 6, the data transmission delay cannot exceed the single-hop propagation delay. Therefore, after the fault recovery, not only the rate decreases but also the maximum supported packet length is reduced. This results in a substantial decline in the network throughput after fault recovery, leading to a decrease in the overall average throughput. According to Figure 8, the end-to-end delivery ratio of the PMAC protocol decreases as the fault probability increases. This is because after a fault occurs, the delivery ratio of PMAC is 0, resulting in a direct decrease in the overall delivery ratio. On the other hand, the end-to-end delivery ratio of RAP-MAC actually increases with the increase in fault rate. This is because after the fault recovery, the rate mode of the entire network changes from three to two, and Mode 2 has a higher transmission success rate, resulting in a higher overall delivery ratio compared to before the fault. In accordance with the proposed algorithm rules, following the recovery from a fault, the rate mode decreases. The lower rate mode has a higher encoding redundancy, which leads to a higher communication success probability, bringing a higher delivery ratio.

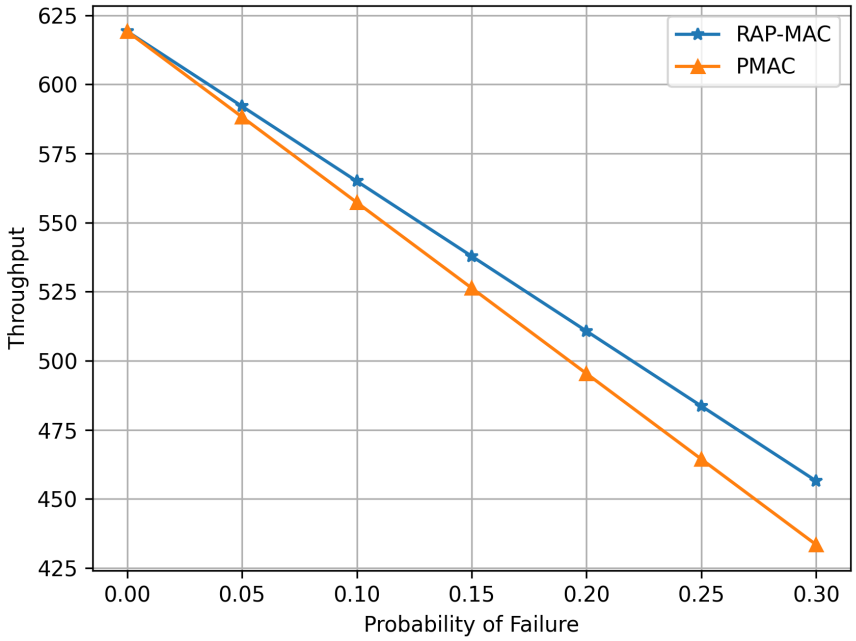

Figure 7. The throughput comparison.

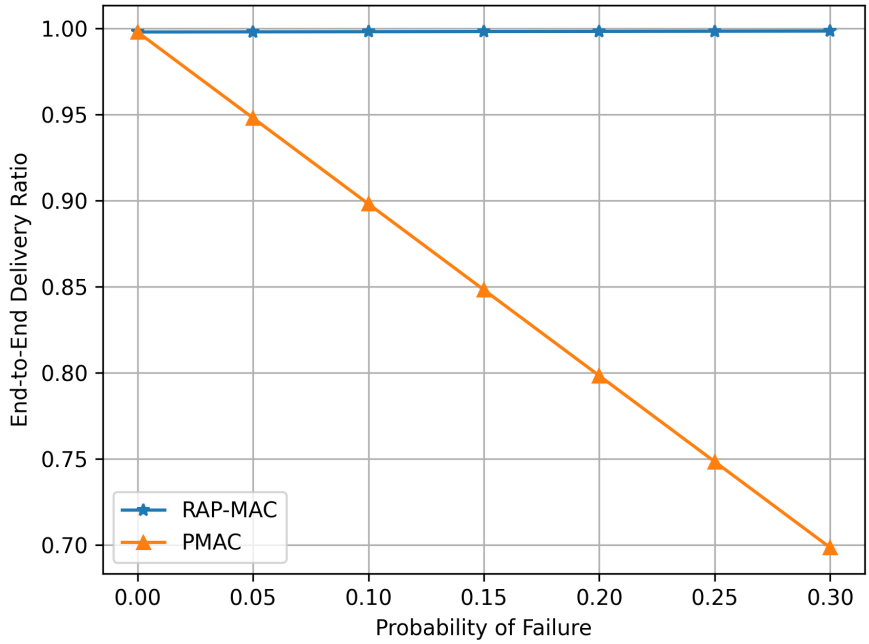

Figure 8. The end-to-end delivery ratio comparison.

5.3. Ocean Experiments

This subsection first provides a brief introduction to the implementation and the deployment of sea trials in two distinct sea areas. Then, the experimental results are analyzed from four aspects—self-regulation, data transmission efficiency, environmental adaptability, and fault recovery capability—to verify the performance of the UA-SN.

(1) Implementation

We encoded the advanced algorithm in SeaLinx, an underwater network protocol stack proposed in [32]. The SeaLinx is implemented in the embedded operating system of underwater acoustic modems. In the ocean experiments, each node is equipped with an integrated bracket composed of an underwater acoustic modem and a battery as shown in Figure 9. The operating frequency of the underwater acoustic modem is 21–27 kHz, with a maximum power of 80 W (190 dB source level). It supports five different data rate modes, including 1047 bps at Mode 1, 2095 bps at Mode 2, 3143 bps at Mode 3, 4191 bps at Mode 4, and 6287 bps at Mode 5, which are determined by the modulation scheme and coding rate. As the data rate increases, the requirements on the underwater environment become more stringent. The adopted acoustic modem is capable of communicating over distances up to 5 km. In the experiment, the RTN continuously transmits data, all RNs actively relay, and the GN receives data. The network throughput calculation at the GN will start when the network entries the phase of stable data transmission. For Mode 1, the data packet size is 600 B; for Mode 2, it is 1250 B; and for Mode 3, it is 1950 B. In addition to the network throughput experiments to verify data transmission efficiency, experiments for environmental adaptability in different sea areas and fault localization detection and network recovery were also conducted to validate the practical flexibility of RAP-MAC.

Figure 9. The underwater acoustic modems.

To thoroughly validate the effectiveness of RAP-MAC in the UA-SN, we conducted experiments in various seas. The first experiment was carried out in June 2021 in the Dalian region of the North China Sea, with depths ranging from 20–50 m and a sea condition level of 3, indicating a challenging underwater environment. The evaluated acoustic field is presented in Figures 10 and 11, where Figure 10 depicts the sound velocity gradient and Figure 11 shows the sound propagation simulation based on Bellhop. In Figures 10 and 11, a negative gradient in sound speed is shown, meaning that sound speed decreases with increasing depth. This causes a noticeable deflection of sound signals towards the seabed. To ensure network connectivity, based on the acoustic field environment, the deployment distance between adjacent nodes was approximately 2 km, resulting in a total end-to-end distance of around 40 km for 21 nodes (as illustrated in Figure 12). Among them, 11 nodes were buoy-mounted (the purple dots in Figure 12), equipped with waterproof boxes containing main control boards and 4G modules for remote operations (as shown in Figure 9), while the remaining ten were mounted on surface boats. This strategy of deployment was adopted to optimize deployment and recovery efficiency in terms of time and cost. Due to severe weather conditions during the experiment, we implemented a zigzag network topology so as to be not too far from the shore. This topology facilitates the longest end-to-end distance and offers easier recovery compared to a straight-line topology. Additionally, to test the network's fault recovery capability, supplementary experiments were conducted in this area, where the SNR, mode, and BLER at communication distances of 3 km and 5 km were tested, with deployment locations detailed in Table 3.

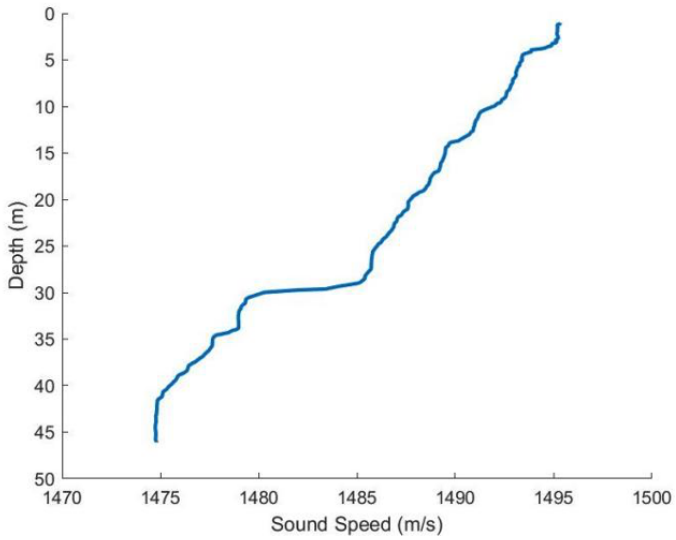

Figure 10. Sound velocity gradient (Underwater sound field (North China Sea)).

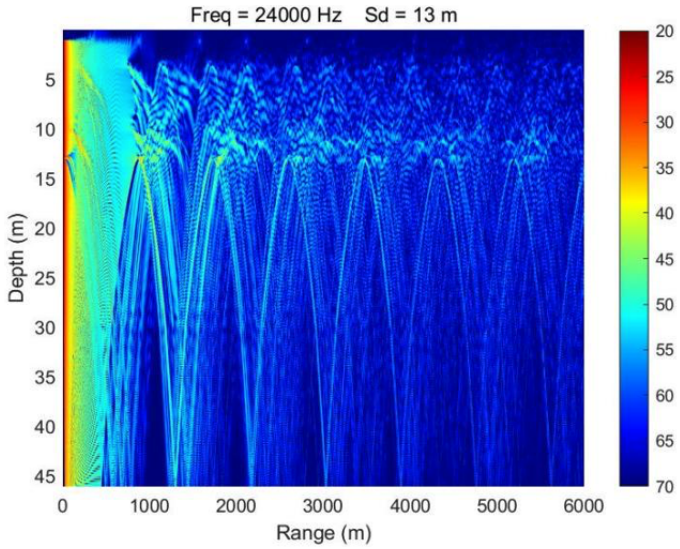

Figure 11. Sound propagation simulation (Underwater sound field (North China Sea)).

Figure 12. Deployment of 21 nodes (North China Sea).

Table 3. The deployment location of trials with different communication range.

		A	B	C
GPS	Longitude	121°38.402′E	121°40.500′E	121°41.823′E
	Latitude	38°51.424′N	38°51.444′N	38°51.387′N
Distance		–	3.03 km	4.94 km

The second experiment was conducted in November 2022 at the Daya Bay of the South China Sea, with depths ranging from 10 to 20 m. Throughout this experiment, the sea conditions maintained as 2, and the sound speed remained relatively constant over depth and time. As depicted in Figure 13, 21 nodes were deployed. Nodes carried by boat were deployed near the coast to significantly reduce the time required for deployment and retrieval. The position of some nodes was adjusted in response to the actual conditions

of the islands and reefs. For nodes 8–17, the average distance between adjacent nodes was 3.5 km, while it was 5.1 km for the remaining nodes. The total distance of end-to-end communication of the 21 nodes was approximately 87 km.

Figure 13. Deployment of 21 nodes (South China Sea).

(2) Experimental Results

(i) The flexible self-regulation

In both sea experiments, 21 nodes were deployed. Owing to the numerous devices and the extensive span of the area, the deployment was conducted in multiple phases, resulting in varied completion times of deployment for nodes at different locations. Compared to PMAC, the algorithm proposed in this study enables the network establishing to be controllable at any time. Upon deployment completion, network establishing process is initiated via the gateway node, which significantly reduces energy consumption caused by this process having started before the deployment of nodes was fully completed. Furthermore, as demonstrated in Table 4, the network's establishing phase offers the advantage of being flexible and controllable. For instance, upon encountering a fault in Node 17, the network was successfully re-established automatically through the gateway node after the fault was rectified. The table indicates that the network fully recovered from the simulated fault in approximately 24 min. Conversely, under PMAC, if a node is removed due to a fault, all nodes must be retrieved and restarted to reset the protocol to its initial state, and then the network can be rebuilt, which is considerably challenging.

Table 4. Fault detection and network recovery (North China Sea).

Fault Node ID	Time of Fault Occurrence	Fault Location	Network Recovery
17	14:37:35	14:47:35	15:01:47

Figures 14–17 illustrate the proposed method can adjust the frequency of transmissions and length of data packet in accordance with the underwater environment. Specifically, Figures 14 and 15 depict the adjustment outcomes from the experiments in Dalian, where the poor sea conditions necessitated increasing the data transmission interval to 160 s and re-

ducing the data length to a single CTD data entry of 30 bytes. Conversely, Figures 16 and 17 detail the adjustments made during the experiments in Daya Bay, where good sea conditions allowed for a reduced data transmission interval of 40 s and an increased data length, transmitting eight CTD data entries at a time. This approach enhances the network's flexibility and controllability, ensuring smooth data transmission across various environments and helping to avert network congestion.

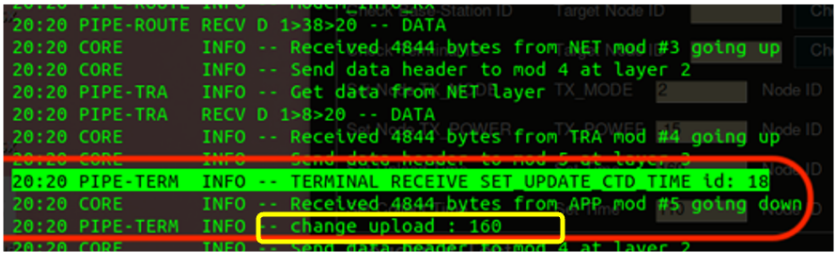

Figure 14. Adjust the transmission interval of RTN (increase: the number 160 in the yellow box represents an interval of 160 s).

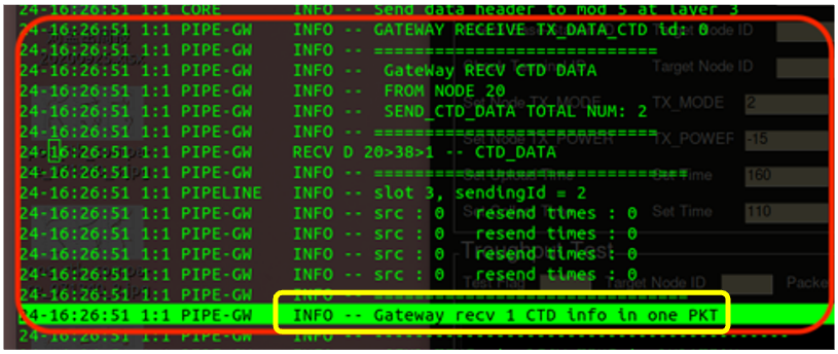

Figure 15. Adjust the packet length of RTN (decrease: the "1 CTD" in the yellow box represents the length of a single CTD data entry of 30 bytes).

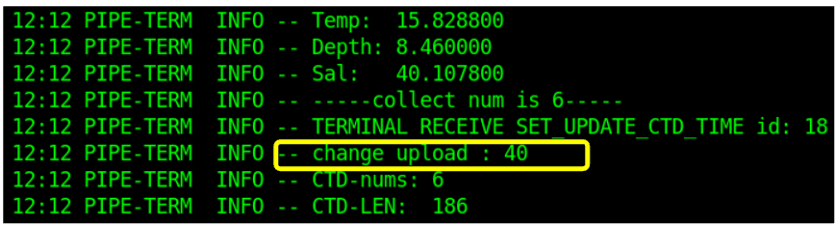

Figure 16. Adjust the transmission interval of RTN (decrease: the number 40 in the yellow box represents an interval of 40 s).

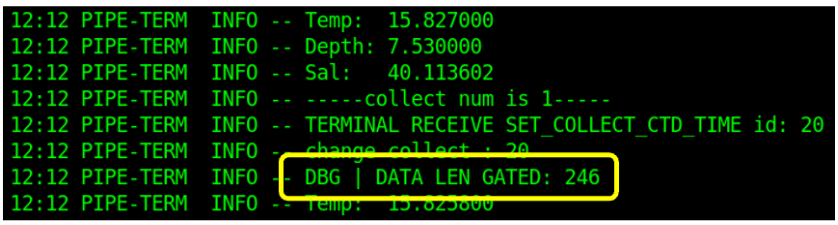

Figure 17. Adjust the packet length of RTN (increase: the number 246 in the yellow box represents the data length of 246 bytes).

(ii) The adaptability to environment and data transmission efficiency

The throughput experiment results in the North China Sea and the South China Sea are detailed in Table 5. In the North Sea experiments, the results of Mode 1 are in line with

the theory. In this deployment scenario, the slot length was 8.3 s, comprising a propagation delay of 1.3 s, a data transmission delay of 6 s, and a guard time of 1 s. Based on the protocol design, the theoretical throughput of the network can be calculated as S = packet length/ 3 × slot length = 600 × 8/(3 × 8.3) = 192.8 bps. This value aligns with the experimental outcomes noted in Table 5. As shown in the table, only Mode 1 was applied for data transmission. The sole utilization of Mode 1 is a consequence of the inherent adaptivity of the protocol that we have proposed. Due to the poor quality of underwater acoustic channel, the network nodes automatically adjusted to the lowest rate mode. In the South Sea experiments, the UA-SN network comprising 21 nodes had an end-to-end communication range of approximately 87 km, with Mode 3 achieving a throughput of 601.6 bps. The slot length under the deployment was around 8.6 s, containing a propagation delay of 3.3 s and a data transmission delay 5.3 s. The theoretical throughput, calculated based on this slot length, is 604.7 bps, closely matching the actual experiment outcomes. The experiment was conducted in a good underwater environment with stable sound speed and good sea conditions, allowing nodes in the UA-SN to adapt to the higher-rate communication of Mode 3.

Table 5. The throughput results.

Parameters		The Number of Nodes	One-Hop Distance	End-to-End Distance	Mode	Throughput
Location	North China Sea	21	2 km	40 km	1	191.6 bps
	South China Sea	21	4.35 km	87 km	3	601.6 bps

The performance, throughput of 601.6 bps over 87 km, is unprecedented in the current published literature, with no reported sea trials of underwater acoustic string networks exceeding this distance and throughput. Furthermore, this result exceeds the recognized upper boundary of underwater acoustic communication experiment performance by 40 km·kbps.

In summary, from the outcomes of the experiments conducted in two distinct areas, it is evident that the proposed protocol is capable of adaptively selecting the optimal mode in response to various underwater conditions and channel qualities, ensuring the network's throughput and reliability. The experiments further validated that RAP-MAC has the capability to independently adapt to the optimal rate mode for the present environment, thus enhancing the efficiency of data transmission.

(iii) The fault recovery capability

Table 4 presents the experimental results that a node failure occurred and the network automatically recovered again after troubleshooting in the North China Sea. The data indicate that replacing the faulty node with backup equipment took a total of 10 min, and approximately 14 min were required from the commencement of network re-establishment to full recovery. Calculations based on the propagation delay and the protocol processing flow of the network establishment phase suggest that successful network establishment without loss packet retransmission would typically require about 7 min. However, due to the poor channel quality during the experiment, there were 18 retransmissions across all hops in the network establishment phase, and then the theoretical time plus retransmission time is consistent with the experiment outcomes.

Due to constraints in the timing of the experiment and the sea conditions, the ability of fault recovery to bypass the faulty node and directly connect to the subsequent hop was not tested. Thus, in the experiment, we instead utilized backup equipment to replace the faulty node's device, followed by network re-establishment. According to the designed fault recovery algorithm, the network adaptively detected and localized the fault and recovered to relay the network re-establishment message to the gateway node, the process of which took about 2 min, significantly less than the time for manual replacement (even in the case that the faulty node's location was known and the test boat was nearby). This

duration would increase substantially if travel time to the site was included, especially for networks deployed in deep-sea environments, where manual replacement becomes even more challenging and time-consuming.

To demonstrate the effectiveness of doubling the communication distance achieved by adjusting the mode and directly connecting to the two-hop node bypassing the faulty one, we conducted tests on different communication modes, SNR and BLER at varying distances during the experiment. The results, displayed in Table 6, include data for communication distances of 3 km and 5 km, with identical transmission power. The table reveals that at the same transmission power, the SNR for the 5 km reception was approximately 3 dB lower than that of 3 km. When Mode 2 was employed at 3 km, the UA-SN 20-hop end-to-end delivery ratio was 95%; correspondingly, at 5 km, Mode 1 could be utilized, achieving a 91% delivery ratio. These findings illustrate that the network fault recovery algorithm, which reduces the rate mode to double the communication distance and skips the faulty node, is effective in practical marine environments, thereby enhancing the entire network's robustness.

Table 6. Performance of communication under different range.

Communication Distance (km)	Average SNR	BLER	Mode	Rate (bps)
5	5.0	0.07	1	1047
3	8.5	0.05	2	2095

5.4. Discussions

In order to verify the performance of RAP-MAC, we conducted simulations and sea trials. The throughput and end-to-end delivery ratio results of the two simulation experiments provided evidence of the practicability of UA-SN in terms of data transmission efficiency, environmental adaptability and fault recovery capability. The above-mentioned network establishment and network parameter adjustment experiments in different sea areas in China demonstrated the flexible self-regulatory ability of UA-SNs in practical environments. The experimental results of a communication distance of 40 km in the Dalian area of the North Sea, with adaptive Mode 1 and a throughput of 191.6 bps, as well as the experimental results of a communication distance of 87 km in the Daya Bay area of the South China Sea, with adaptive Mode 3 and a throughput of 601.6 bps, validated the adaptability and data transmission efficiency of UA-SNs to changes in actual marine environments. The comprehensive results of network failure recovery experiments in the above-mentioned sea trials, and the experiments on SNR, BLER, and rate mode under the condition of doubling the communication distance, verified the fault recovery capability of UA-SNs in real scenarios, thereby improving the robustness of the network.

The proposed MAC protocol is specifically aimed at a single-string network scenario, which is effective in resolving discontinuous node failures in UA-SNs. Nevertheless, if there are consecutive failures with two or more nodes, the algorithm will be unable to resolve the problem because of physical communication constraints. Extending the network from a single-string configuration to a dual or multistring architecture can expand the coverage area and increase the communication distance. In the event of a node failure in one string, the immediate upstream node can create links with nodes in neighboring strings to guarantee the data transmission. This augmentation improves network resilience and elevates overall network robustness.

6. Conclusions

Underwater acoustic string networks play a critical role in long-distance data transmissions in deep-sea and shallow-water environments. To meet the requirements of underwater applications in real-world scenarios, we propose a robust and adaptive pipeline MAC protocol. The protocol design features four highlights. (1) Efficiency: adopt a time scheduling concurrency algorithm to improve network throughput. (2) Self-regulatory abil-

ity: optimize network scalability through real-time slot allocations, and dynamically adjust data transmission frequency and length to prevent congestion in poor channel conditions. (3) Environmental adaptability: combine the MAC layer and the physical layer to perform cross-layer optimization, adaptively selecting the optimal rate based on real-time SNR information, to address the impacts of the temporal and spatial dynamics of underwater acoustic channels. (4) Fault recovery capability: design an adaptive fault detection and recovery algorithm to ensure the continuous operation of the UA-SN in the event of a node failure, hence enhancing network resilience. Through the simulation comparison experiments with PMAC, the environmental adaptability and fault recovery ability of RAP-MAC are confirmed, highlighting its robustness. Through sea experiments in different sea areas of Northern and Southern China, the effectiveness of RAP-MAC has been fully verified from the above four perspectives. The sea trial result of UA-SN communication with a throughput of 601.6 bps over 87 km is unprecedented in the current published literature, except for the network systems built by the US Navy. This achievement exceeds the upper bound of underwater acoustic communication test performance by 40 km·kbps.

In order to further enhance the resilience of underwater acoustic string networks and expand the network coverage area, we plan to conduct research on the multistring underwater acoustic network and their protocols in the future.

Author Contributions: Conceptualization, X.P. and M.L.; methodology, X.P.; software, X.P., M.L. and J.Z.; validation, X.P., M.L., J.Z. and L.H.; formal analysis, X.P.; investigation, X.P.; resources, J.-H.C. and J.L.; data curation, X.P. and Z.P.; writing—original draft preparation, X.P.; writing—review and editing, X.P. and Z.P.; visualization, X.P. and M.L.; supervision, Z.P.; project administration, J.-H.C.; funding acquisition, J.-H.C. and J.L. All authors have read and agreed to the published version of the manuscript.

Funding: This work was supported in part by the National Natural Science Foundation of China under Grant 61971206 and Grant 62101211; in part by Overseas Top Talents Program of Shenzhen under Grant KQTD20180411184955957 and Grant LHTD20190004; and in part by the National Key Research and Development Program under Grant 2021YFC2803000 and Grant 2022YFC2803800.

Data Availability Statement: The data presented in this paper are available via contacting the corresponding author.

Conflicts of Interest: Author Jun-Hong Cui was employed by the company Smart Ocean Technology. The remaining authors declare that the research was conducted in the absence of any commercial or financial relationships that could be construed as a potential conflict of interest.

References

1. Chaudhary, M.; Goyal, N.; Benslimane, A.; Awasthi, L.K.; Alwadain, A.; Singh, A. Underwater wireless sensor networks: Enabling technologies for node deployment and data collection challenges. *IEEE Internet Things J.* **2022**, *10*, 3500–3524. [CrossRef]
2. Li, J.; Wu, J.; Li, C.; Yang, W.; Bashir, A.K.; Li, J.; Al-Otaibi, Y.D. Information-centric wireless sensor networking scheme with water-depth-awareness content caching for underwater IoT. *IEEE Internet Things J.* **2021**, *9*, 858–867. [CrossRef]
3. Haque, K.F.; Kabir, K.H.; Abdelgawad, A. Advancement of routing protocols and applications of underwater wireless sensor network (UWSN)—A survey. *J. Sens. Actuator Netw.* **2020**, *9*, 19. [CrossRef]
4. Fattah, S.; Gani, A.; Ahmedy, I.; Idris, M.Y.I.; Targio Hashem, I.A. A survey on underwater wireless sensor networks: Requirements, taxonomy, recent advances, and open research challenges. *Sensors* **2020**, *20*, 5393. [CrossRef] [PubMed]
5. Murad, M.; Sheikh, A.A.; Manzoor, M.A.; Felemban, E.; Qaisar, S. A survey on current underwater acoustic sensor network applications. *Int. J. Comput. Theory Eng.* **2015**, *7*, 51. [CrossRef]
6. Kumar, P.; Kumar, P.; Priyadarshini, P.; Srija. Underwater acoustic sensor network for early warning generation. In Proceedings of the 2012 Oceans, Hampton Roads, VA, USA, 14–19 October 2012; pp. 1–6.
7. Kerfoot, W.C.; Hobmeier, M.M.; Swain, G.; Regis, R.; Raman, V.K.; Brooks, C.N.; Grimm, A.; Cook, C.; Shuchman, R.; Reif, M. Coastal Remote Sensing: Merging Physical, Chemical, and Biological Data as Tailings Drift onto Buffalo Reef, Lake Superior. *Remote Sens.* **2021**, *13*, 2434. [CrossRef]
8. Felemban, E.; Shaikh, F.K.; Qureshi, U.M.; Sheikh, A.A.; Qaisar, S.B. Underwater sensor network applications: A comprehensive survey. *Int. J. Distrib. Sens. Netw.* **2015**, *11*, 896832. [CrossRef]
9. Ali, S.; Ashraf, A.; Qaisar, S.B.; Afridi, M.K.; Saeed, H.; Rashid, S.; Felemban, E.A.; Sheikh, A.A. SimpliMote: A wireless sensor network monitoring platform for oil and gas pipelines. *IEEE Syst. J.* **2016**, *12*, 778–789. [CrossRef]

10. Du, X.; Liu, X.; Su, Y. Underwater acoustic networks testbed for ecological monitoring of Qinghai Lake. In Proceedings of the OCEANS 2016-Shanghai, Shanghai, China, 10–13 April 2016; pp. 1–4.
11. Jiang, S. State-of-the-art medium access control (MAC) protocols for underwater acoustic networks: A survey based on a MAC reference model. *IEEE Commun. Surv. Tutorials* **2017**, *20*, 96–131. [CrossRef]
12. Chen, W.; Guan, Q.; Yu, H.; Ji, F.; Chen, F. Medium access control under space-time coupling in underwater acoustic networks. *IEEE Internet Things J.* **2021**, *8*, 12398–12409. [CrossRef]
13. Qiao, G.; Yang, J.; Ma, X.; Zhang, Y.; Dong, H. Simulation and experimental verification of MAC protocols for underwater acoustic communication networks. In Proceedings of the 8th International Conference on Underwater Networks & Systems, Kaohsiung, Taiwan, 11–13 November 2013; pp. 1–5.
14. Cui, J.H.; Kong, J.; Gerla, M.; Zhou, S. The challenges of building mobile underwater wireless networks for aquatic applications. *IEEE Netw.* **2006**, *20*, 12–18.
15. Cui, J.H.; Kong, J.; Gerla, M.; Zhou, S. Challenges: Building scalable and distributed Underwater Wireless Sensor Networks (UWSNs) for aquatic applications. *Channels* **2005**, *45*, 22–35.
16. Le, S.N.; Zhu, Y.; Peng, Z.; Cui, J.H.; Jiang, Z. PMAC: A real-world case study of underwater MAC. In Proceedings of the 8th International Conference on Underwater Networks & Systems, Kaohsiung, Taiwan, 11–13 November 2013; pp. 1–8.
17. Al Guqhaiman, A.; Akanbi, O.; Aljaedi, A.; Chow, C.E. A survey on MAC protocol approaches for underwater wireless sensor networks. *IEEE Sens. J.* **2020**, *21*, 3916–3932. [CrossRef]
18. Chen, K.; Ma, M.; Cheng, E.; Yuan, F.; Su, W. A survey on MAC protocols for underwater wireless sensor networks. *IEEE Commun. Surv. Tutorials* **2014**, *16*, 1433–1447. [CrossRef]
19. Luque-Nieto, M.Á.; Moreno-Roldán, J.M.; Otero, P.; Poncela, J. Optimal scheduling and fair service policy for STDMA in underwater networks with acoustic communications. *Sensors* **2018**, *18*, 612. [CrossRef] [PubMed]
20. Lmai, S.; Chitre, M.; Laot, C.; Houcke, S. Throughput-efficient super-TDMA MAC transmission schedules in ad hoc linear underwater acoustic networks. *IEEE J. Ocean. Eng.* **2016**, *42*, 156–174. [CrossRef]
21. Yang, J.; Qiao, G.; Hu, Q.; Zhang, J.; Du, G. A dual channel medium access control (MAC) protocol for underwater acoustic sensor networks based on directional antenna. *Symmetry* **2020**, *12*, 878. [CrossRef]
22. Bai, W.; Motani, M.; Wang, H. On the throughput of linear unicast underwater networks. In Proceedings of the GLOBECOM 2017—2017 IEEE Global Communications Conference, Singapore, 4–8 December 2017; pp. 1–6.
23. Peng, Z.; Zhou, Z.; Cui, J.H.; Shi, Z.J. Aqua-Net: An underwater sensor network architecture: Design, implementation, and initial testing. In Proceedings of the OCEANS 2009, Biloxi, MS, USA, 26–29 October 2009; pp. 1–8.
24. Mo, H.; Pu, L.; Zhu, Y.; Peng, Z.; Jiang, Z.; Cui, J.H. Evaluating selective ARQ and slotted handshake based access in real world underwater networks. In Proceedings of the Wireless Algorithms, Systems, and Applications: 8th International Conference, WASA 2013, Zhangjiajie, China, 7–10 August 2013; Proceedings 8; Springer: Berlin/Heidelberg, Germany, 2013; pp. 206–220.
25. Pu, L.; Luo, Y.; Mo, H.; Le, S.; Peng, Z.; Cui, J.H.; Jiang, Z. Comparing underwater MAC protocols in real sea experiments. *Comput. Commun.* **2015**, *56*, 47–59. [CrossRef]
26. Rice, J.; Creber, B.; Fletcher, C.; Baxley, P.; Rogers, K.; McDonald, K.; Rees, D.; Wolf, M.; Merriam, S.; Mehio, R.; et al. Evolution of seaweb underwater acoustic networking. In Proceedings of the OCEANS 2000 MTS/IEEE Conference and Exhibition. Conference Proceedings (Cat. No. 00CH37158), Providence, RI, USA, 11–14 September 2000; Volume 3, pp. 2007–2017.
27. Rice, J.; Green, D. Underwater acoustic communications and networks for the us navy's seaweb program. In Proceedings of the 2008 Second International Conference on Sensor Technologies and Applications (Sensorcomm 2008), Cap Esterel, France, 25–31 August 2008; pp. 715–722.
28. Grund, M.; Freitag, L.; Preisig, J.; Ball, K. The PLUSNet underwater communications system: Acoustic telemetry for undersea surveillance. In Proceedings of the OCEANS 2006, Boston, MA, USA, 18–21 September 2006; pp. 1–5.
29. Ma, L.; Qiao, G.; Liu, S. Heu OFDM-modem for underwater acoustic communication and networking. In Proceedings of the 9th International Conference on Underwater Networks & Systems, Rome, Italy, 12–14 November 2014; pp. 1–5.
30. Nguyen, N.T.; Heldal, R.; Lima, K.; Oyetoyan, T.D.; Pelliccione, P.; Kristensen, L.M.; Hoydal, K.W.; Reiersgaard, P.A.; Kvinnsland, Y. Engineering Challenges of Stationary Wireless Smart Ocean Observation Systems. *IEEE Internet Things J.* **2023**, *10*, 14712–14724. [CrossRef]
31. Zhu, Y.; Le, S.; Pu, L.; Lu, X.; Peng, Z.; Cui, J.H.; Zuba, M. Aqua-Net Mate: A real-time virtual channel/modem simulator for Aqua-Net. In Proceedings of the 2013 MTS/IEEE OCEANS-Bergen, Bergen, Norway, 10–14 June 2013; pp. 1–6.
32. Le, S.N.; Peng, Z.; Cui, J.H.; Zhou, H.; Liao, J. Sealinx: A multi-instance protocol stack architecture for underwater networking. In Proceedings of the 8th International Conference on Underwater Networks & Systems, Kaohsiung, Taiwan, 11–13 November 2013; pp. 1–5.